This is a previous version of the article published in Construction and Building Materials. 2020, 249: 118713. https://doi.org/10.1016/j.conbuildmat.2020.118713

Non-linear multivariable model for predicting the steel to concrete bond after high temperature exposure

F.B. Varona[a], F.J. Baeza[a], D. Bru[a], S. Ivorra[a,1]

[a] Department of Civil Engineering, University of Alicante, Alicante, Spain.

[1] Corresponding author: sivorra@ua.es

Abstract

The bond mechanism between steel and concrete can be compromised during a fire and is one of the least investigated phenomena in concrete research. In this work we present a thorough review of the experimental data available on this topic. The results from the tests reported by a number of researchers have been systematically collected in a database. This work also reports the results obtained in the bond strength tests carried out on four batches of normal and high strength concretes exposed to temperatures up to 825 °C. The database provides the source for a multiple regression analysis which is performed in order to define a model aimed at predicting the bond strength as a function of several variables: the exposure temperature, the concrete compressive strength at ambient temperature, the type of fibre addition, the fibre volume fraction, the age at testing, the bond length and the concrete cover of the steel bar. Based on different error measurements, our model is favourably compared to the set of experimental results reported here and also other prediction models reported in the literature.

Keywords: bond strength; pull-out strength; fibre reinforced concrete; high performance concrete; high temperature

1. Introduction

The behaviour of concrete exposed to high temperature has been thoroughly researched during the 20th century. One of the earliest pieces of research dates from 1920 [1]. The effects of the exposure of concrete to elevated temperatures can be described through the following stages [2]: (i) drying of capillary water occurs between 20 and 100 °C, with a slight reduction of the compressive strength; (ii) for temperatures up to 300 °C an increase of the compressive strength is reported for young and dry concretes; (iii) the dehydration of the Calcium-Silicate-Hydrate gel starts around 150-180 °C and the dehydration of the portlandite takes place between 400 and 600 °C; (iv) a notorious drop of the mechanical properties of concrete is observed in the interval 300-650 °C; (v) in the case of quartzitic aggregates, a transformation of α-quartz into β-quartz takes place at 570 °C and entails a volumetric increase which is thought to be responsible for the higher drop of mechanical properties in concretes made with this type of aggregates as compared to other types; (vi) the decarbonation of limestone aggregates occurs between 600 and 900 °C; (vii) by 700 °C the dehydration of the CSH gel is mostly complete; (viii) the rate of reduction of mechanical properties slows down for temperatures higher than 650 °C; (ix) melting of some types of aggregates takes place at around 1200 °C and melting of the Portland cement paste is reported at around 1350 °C.

Research on the performance of high strength concrete (HSC) at high temperatures was carried out since the late 1970's. Their compact microstructure makes HSC more sensitive to the sloughing off or even the explosive spalling of the concrete cover in the hottest elements [3]–[8]. The causes of thermal spalling have been discussed in a number of reports: (i) heating rate [2]; (ii) incompatibility of thermal strains of components (cement paste, aggregates, steel) or layers with different temperatures and coefficients of thermal expansion [9], [10]; (iii) pore pressure build up caused by steam expelled in the dehydration of the CSH gel and the portlandite [2] and also by the CO_2 expelled in the calcination of limestone aggregates [11]. The behaviour of fibre reinforced concretes exposed to fire temperatures has also been studied [12]–[18] and some prediction models have been created for a number of mechanical properties –compressive strength, tensile strength, elastic modulus, stress-strain relationship– for both polypropylene fibre [19] and steel fibre [20] reinforced concretes.

Concrete fire design is covered by international standards, such as the Model Code 2010 [21] and the Eurocode 2 [22]. These documents present simplified and advanced analysis methods, based on tabulated data and curves that describe the evolution of mechanical and thermal properties of concrete and steel. However, these standards do not provide models for the evolution of the bond strength between the steel reinforcement and the concrete during or after exposure to elevated temperatures. Compared to other mechanical properties, steel to concrete bond after high temperature exposure may be one of the least investigated phenomena in concrete research.

This paper presents an exhaustive review of the state of the art concerning the study of steel to concrete bond at high temperature. Some authors have used their own experimental data to propose analytical expressions to predict the peak bond strength and to adapt the formulation which is given in Model Code 2010. Many models treat the residual peak bond strength as a function of the exposure temperature only. All the experimental results reported in the literature review are used here to develop a linear multiple regression analysis to study how other independent variables affect the bond at high temperature. Additionally, we have carried out further bond strength tests on four batches of normal and high strength concretes and the results are then compared with the multivariable models developed. In the discussion, several error measurements are used to compare the new multivariable models with the ones reported by other authors and described in our review.

2. Literature review

2.1 Previous experimental studies

At the moment of writing this paper, the available pieces of research that have reported experimental results on the loss of steel-to-concrete bond at high temperature are the following: Milovanov and Salmanov [23], Kasami et al. [24], Reichel [25], Diederichs and Schneider [26], Hertz [27], Morley and Royles [28], Ahmed et al. [11], Haddad and Shannis [29], Haddad et al. [30], Bingöl and Gül [31], Arel and Yazici [32], Ergün et al. [33], Lublóy and Hlavička [34], Varona et al. [35],

Lee et al. [36] and Yang et al. [37]. Table 1 summarises the main parameters and conditions studied in these references.

There is no unique standard to test the bond strength between steel and concrete and there is also no uniform procedure to test material properties at elevated temperatures. Many of these studies have been based in the RILEM/CEB/FIP pull-out test or a modification suggested in [38]; although the original shape of the pull-out specimens is cubic, many studies used cylindrical specimens but maintained the standard's size ratios (e.g., size of specimen to bar diameter ratio, bond length to bar diameter ratio). Some studies used other geometries, such as conical [27] and prismatic including additional transverse reinforcement [30]. This lack of uniformity affects two parameters that are critical for the bond strength: the bond length and the concrete cover. The Model Code 2010 [21] defines the local bond stress-slip relationship represented in Fig. 1, which is valid for ribbed bars under good bond condition and with values concrete cover equal or greater than five times the bar diameter. With smaller covers, the brittle splitting failure may develop instead of the pull-out failure (this phenomenon was one of the objectives in [32]). Also, according to [38], in for the pull-out tests to reproduce the local bond stress-slip law, the ratio of bond length to bar diameter should be limited. As mentioned above, these parameters show important variations in the reported studies. Furthermore, some of the earlier studies included both plain bars and ribbed bars.

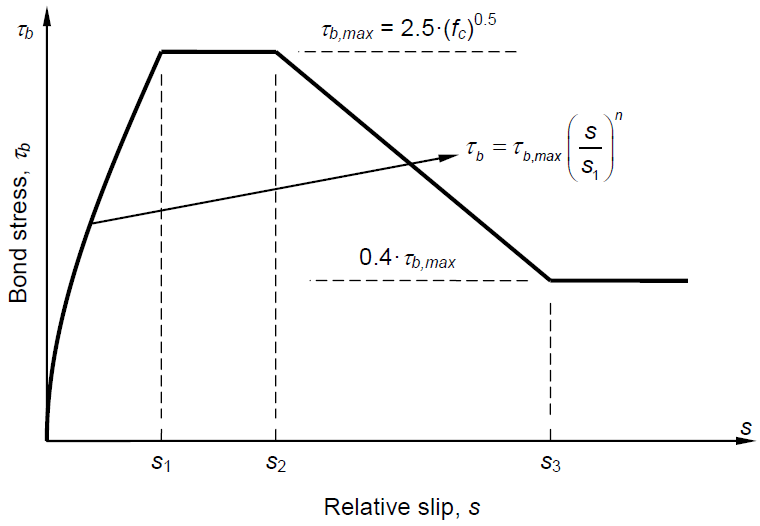

Fig. 1 Bond stress-slip relationship in Model Code 2010 [21]

The range of concrete compressive strength varies from 19 to 98 MPa, thus covering both normal strength concretes (NSC) and high strength concretes. It may be noted in Table 1 that the original compressive strength at ambient temperature was not always measured or reported. Regarding the composition of the concrete, some studies reported the use of admixtures and the maximum aggregate sizes, although this information is not given in several references. The same happens with the aggregate type, which was not always reported. Some of the most recent studies also included fibre

addition, including polypropylene fibres, steel fibres or a mix of both of them (hybrid fibre). The age at testing also varied from one study to another: the extreme cases are reported in [11], with tests at 7 and 35 days, and in [26], with tests at 150 and 600 days.

Table 1. Summary of literature review, part 1

Reference	Strength grade	$f_{c,cube,20\,°C}$ [MPa]	Fibres	Volume fraction	Type of aggregate	Admixture	Admixture content	Specimen geometry
Milovanov and Salmanov [23]	NSC		-	0%	?	-	-	Prism. 140 mm
Kasami et al. [24]	NSC		-	0%	S NC	-	-	?
Reichel [25]	NSC		-	0%	S	-	-	Prism. 150 mm RC
Diederichs and Schneider [26]	NSC HSC	54	-	0%	S	-	-	Cyl. 172 mm
Hertz [27]	NSC	20	-	0%	S C	-	-	Conical 150 mm
Morley and Royles [28]	NSC	35	-	0%	?	-	-	Cyl. 126 mm
Ahmed et al. [11]	NSC		-	0%	C	-	-	Prism. 150 mm
Haddad and Shannis [29]	HSC	66-73	-	0%	C	NP	0-25%	Cyl. 82 mm
Haddad et al. [30]	HSC	77-104	- S S+PP BCS A+BCS	0% 2% 2% 2% 2%	B	-	-	Prism. 100 mm RC
Bingöl and Gül [31]	NSC	25-45	-	0%	S	-	-	Cyl. 100 mm
Arel and Yazici [32]	NSC	29-75	-	0%	C	- SF	- 11%	Cub. 150 mm
Ergün et al. [33]	NSC	22-48	-	0%	C	FA	16-25%	Cyl. 150 mm
Lublóy and Hlavička [34]	NSC HSC	46-75	- S PP	0% 0.45% 0.11%	S LW	-	-	Cyl. 120 mm
Varona et al. [35]	NSC HSC	19-98	PP S+PP	0.16% 0.27% 0.41% 0.52%	C	- SF	- 10%	Cyl. 125 mm
Lee et al. [36]	NSC	21	-	0%	S	-	-	Cyl. 102 mm
Yang et al. [37]	NSC	48	-	0%	S	-	-	Cub. 200 mm RC

Strength grade: normal strength concrete, NSC; high strength concrete, HSC. Fibres: steel, S; polypropylene, PP; brass coated steel, BCS. Type of aggregate: calcareous, C; siliceous, S; basalt, B; non-conventional, NC; lightweight, LW. Admixture: silica fume, SF; fly ash, FA. Specimen geometry: including reinforcing bars, RC.

Table 1. Summary of literature review, part 2

Reference	Length to diameter	Cover to diameter	Type of bar	Age at testing [d.]	Heating	Max. T [°C]	Time at max. T [h]	Cooling	Type of test
Milovanov and Salmanov [23]	15	3.00	P R	28 (?)	E	450	?	N	RU
Kasami et al. [24]	?	?	P	90	E	300	2160	N	RU
Reichel [25]	32.14	4.86	P R	28 (?)	F	600	-	N	RU
Diederichs and Schneider [26]	5.00	4.88	P R W	150 600	E	800	3	No	S U
Hertz [27]	6 9.38 12.5	2.5 4.19 5.75	R	?	E	800	2	N	RU
Morley and Royles [28]	2.00	3.44	P R	90	E	750	1	N	S RU
Ahmed et al. [11]	12.50	5.75	R	7 35	E	600	1 2	N I	RU
Haddad and Shannis [29]	8.33	1.78	R	40	E	800	1	N	RU
Haddad et al. [30]	7.5	2	R	35	E	700	2	N	RU
Bingöl and Gül [31]	7.5 12.5 20	5.75	R	28	E	700	3	N I	RU
Arel and Yazici [32]	5	2.86 3.93 5.00	R	28	E	500	3	N	RU
Ergün et al. [33]	12.50 15.63 20.83	3.25 4.19 5.75	P R	90	E	800	0.75	N	RU
Lublóy and Hlavička [34]	3.33	4.5	R	28	E	800	2	N	RU
Varona et al. [35]	4.17	4.71	R	60	E	825	1.25	N	RU
Lee et al. [36]	5.35	4.85	R	28	E	800	2	N I	RU
Yang et al. [37]	2	4.50	R	60	E	800	3	N	RU

Type of bar: plain, P; ribbed, R; prestressing wire, W. Heating: electrical furnace, E; fire exposure, F. Cooling: natural air cooling, N; water immersion, I. Type of test: residual unstressed, RU; stressed at high temperature, S; unstressed at high temperature, U.

Regarding the thermal treatment, electrical furnaces were used in most cases, with heating rates in the range of 1 to 10 °C/min, slower than the standard time-temperature curve for fire tests on building materials and structures. The maximum exposure temperature was maintained during a period of time in order to thermally saturate the specimens with a homogeneous distribution of temperatures. The duration of this thermal saturation plateau is the parameter with the widest range of values (from 45

minutes to 90 days) However, real fire exposure was actually conducted in [25]. Also, in most cases, the pull-out tests were carried out after cooling to ambient temperature, which is expected to cause a greater loss of mechanical properties, including the bond strength, as concluded in [11], [28], [31].

2.2 Prediction models for bond at high temperature

Some of these references have developed analytical models for the residual bond strength after exposure to elevated temperatures. These models have been collected in Table 2. Most of these models were developed through regression analysis based on their authors' own experimental results. Haddad and Shannis [29] proposed two models based on their experiments on high strength concretes (HSC): one of them was based on the natural pozzolan content and a second one was for general use and is presented here as Eq. [1], which makes the normalised residual bond strength (*NRBS*) to depend on the normalised residual compressive strength of concrete (*NRCS*) after exposure to high temperature. The experiments on the bond strength to fibre reinforced high strength concretes (FRHSC) which were carried out by Haddad et al. [30] yielded the analytical model in Eq. [2], in which T is the exposure temperature and coefficient k takes the following values: 152 for plain concrete; 170 for FRC with hook-end steel fibres and also for FRC with a mixture of hook-end steel fibres and high performance polypropylene fibres; 159 for FRC with a mixture of hook-end steel fibres and brass coated steel fibres; and 149 for FRC with brass coated steel fibres. The models developed by Aslani and Samali [39] are the only models in Table 2 to be based on a wide array of previously reported experimental results ([11], [26]–[31]). Both a simplified model (Eq. [3]-[4]) and a slightly more advanced model (Eq. [5]) were devised. The former is limited to the temperature range from 20 to 800 °C and depends on the type of cooling, the exposure temperature T and the bond length l. In the latter (Eq. [5]), $f_{c,T}$ is the cylinder compressive strength after exposure to temperature T and $f_{c,20\,°C}$ is the cylinder compressive strength at ambient temperature. This second model is limited to temperatures from 100 to 800 °C. For the ratio ($f_{c,T}$ / $f_{c,20\,°C}$), the authors gave a set of equations covering normal strength concrete (NSC), high strength concrete (HSC), calcareous aggregate concrete and lightweight aggregate concrete. In the model by Arel and Yazici [32] –based on their experiments on NSC and HSC– P_t is the pull-out force (in kN) for a 14-mm-diameter deformed steel bar, c is the thickness of the concrete cover, and f_{c28}, f_{ct28} and E_{c28} are the compressive strength, splitting tensile strength and modulus of elasticity of concrete, respectively, all of which correspond to an age of 28 days and at ambient temperature. Ergün et al. [33] used their experimental data on plain NSC to propose the formulation in Eq. [7]-[8]. In their work based on fibre reinforced NSC and HSC, Varona et al. [35] used their own experimental results to propose several equations for different types of concretes. The two models shown in Table 2 correspond to NSC (Eq. [9]) and HSC (Eq. [10]). However, in both cases the concrete mixes included a very small amount of monofilament polypropylene fibres to avoid explosive spalling.

Table 2. Analytical models for the steel-concrete bond strength at high temperature

Reference	Equation	Source
Haddad and Shannis [29]	$NRBS = 0.0104 \cdot \left(NRCS\right)^{2.02}$ [1]	[29]
Haddad et al. [30]	$NRBS = k\dfrac{1-\left(-0.0035\cdot\sqrt{T}-0.52\right)^2}{1+\left(-0.0035\cdot T-0.52\right)^2}$ [2]	[30]
Aslani and Samali [39]	Simplified method, natural air cooling: $NRBS = \begin{cases} 100-0.033\cdot T-1\cdot10^{-4}\cdot T^2 & 30\text{ mm} < l \le 100\text{ mm} \\ 100-0.082\cdot T-2\cdot10^{-5}\cdot T^2 & 100\text{ mm} < l \le 160\text{ mm} \\ 100-0.06\cdot T-7\cdot10^{-5}\cdot T^2 & 30\text{ mm} \le l \le 160\text{ mm} \end{cases}$ [3] Simplified method, cooling by water immersion: $NRBS = \begin{cases} 100-0.015\cdot T-1\cdot10^{-4}\cdot T^2 & 30\text{ mm} < l \le 100\text{ mm} \\ 100-0.090\cdot T-2\cdot10^{-5}\cdot T^2 & 100\text{ mm} < l \le 160\text{ mm} \\ 100-0.047\cdot T-7\cdot10^{-5}\cdot T^2 & 30\text{ mm} \le l \le 160\text{ mm} \end{cases}$ [4] Alternative model: $NRBS = \begin{cases} 105.38\cdot\left(f_{c,T}/f_{c,20\,°C}\right)-2.55 & 30\text{ mm} < l \le 100\text{ mm} \\ 52.73\cdot\left(f_{c,T}/f_{c,20\,°C}\right)+41.69 & 100\text{ mm} < l \le 160\text{ mm} \\ 79.05\cdot\left(f_{c,T}/f_{c,20\,°C}\right)+18.62 & 30\text{ mm} \le l \le 160\text{ mm} \end{cases}$ [5]	[11], [26]–[31]
Arel and Yazici [32]	$P_t = 68.4-\dfrac{7520}{84+f_{c28}+f_{ct28}+E_{c28}+c}-0.0258\cdot T$ [6]	[32]
Ergün et al. [33]	Deformed steel bar with yield strength of 420 MPa: $NRBS = 102.3-0.00268\cdot T-8.21\cdot10^{-5}\cdot T^2$ [7] Deformed steel bar with yield strength of 500 MPa: $NRBS = 90.5-0.0352\cdot T-6.29\cdot10^{-5}\cdot T^2$ [8]	[33]
Varona et al. [35]	Normal strength concrete: $\tau_{b,max,T} = 0.354\cdot f_{c,cub,T}-0.15$ with $\dfrac{f_{c,cub,T}}{f_{c,cub,20\,°C}} = 1+0.000248\cdot T-1.54\cdot10^{-6}\cdot T^2 \not< 0$ [9] High strength concrete: $\tau_{b,max,T} = 0.393\cdot f_{c,cub,T}-3.43$ with $\dfrac{f_{c,cub,T}}{f_{c,cub,20\,°C}} = 1.01-0.000103\cdot T-1.06\cdot10^{-6}\cdot T^2 \not< 0$ [10]	[35]
Yang et al. [37]	$\tau_{b,max,T} = \beta\cdot\sqrt{f_{c,cub,T}}$ with $f_{c,cub,T} = f_{c,cub,20\,°C}-0.05\cdot T$ [11]	[37]

In Eq. [9]-[10], $\tau_{b,max,T}$ is the peak bond strength after exposure to temperature T, $f_{c,cub,T}$ is the cube compressive strength after exposure to temperature T, and $f_{c,cub,20\,°C}$ is the cube compressive strength

at ambient temperature. Finally, the work by Yang et al. [37] tested the bond between slightly corroded steel bars and concrete after high temperature exposure. The authors developed an analytical model which attempted a generalisation of the bond stress-slip relationship in Model Code 2010 [21]. The influence of the mass loss due to corrosion affected the residual bond stress as a function of the relative steel-to-concrete slip. However, the peak bond strength was not found to depend on the loss mass and the authors developed the model given in Eq. [11], where the value of coefficient β can be taken as 3.5 with exposure temperatures up to 400 °C, and as 2.5 in the range from 600 to 800 °C.

3. Methodology

3.1 Database with experimental results in the state of the art

Table 1 summarises the most significant variables of the studies on steel to concrete bond at high temperatures which have been described in this paper's literature review section. The experimental results reported by those studies have been collected in a database. These data are represented in Fig. 2 as a function of temperature only. The vertical axis represents the normalised residual bond strength (*NRBS*), i.e., the ratio between the residual bond strength after high temperature exposure and the original value at ambient temperature, expressed as a percentage. This ratio is expressed as a percentage. The total number of data points available is 450, 374 of which correspond to temperatures between 50 and 825 °C –76 points with *NRBS* = 100% are superimposed at 20 °C.

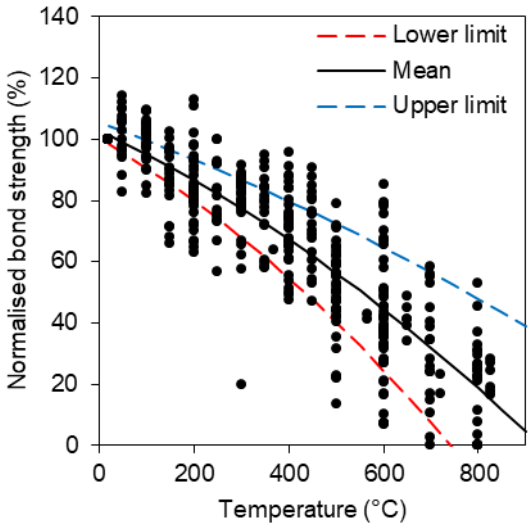

Fig. 2 Bond strength as a function of temperature: 466 experimental data points and non-linear simple regression with 95% confidence interval

The most striking feature of the data shown in Fig. 2 is the great dispersion exhibited at some temperatures, especially at 600 °C. This dispersion may be explained by a number of parameters that also affect the phenomenon and are annotated in Table 1: compressive strength at ambient

temperature, content and type of fibres, content and type of admixture, type of aggregate, aggregate size distribution, specimen geometry and size, bond length, concrete cover, type of bar, age at testing, heating device, duration of thermal saturation plateau, cooling procedure, and type of test.

An example of the database is shown in Table 3. Some of the aforementioned variables affecting bond have not been reported in all previous studies (e.g., type of aggregate, aggregate size). Therefore, eight independent variables and three dependent variables have been identified for each of the experiments reported in the database, based on the available reported information. The independent variables in the database are the following:

- Type of fibre: this is a categorical variable that adopts the value 0 when there is no fibre content, 1 when steel fibres are used, 2 when polypropylene fibres are used, and 3 when hybrid fibres are added to the concrete.
- Fibre content expressed as percentage of volume fraction (*VF*).
- Concrete compressive strength at ambient temperature ($f_{c,20\,°C}$, expressed in MPa). Values measured in cubic specimens have been transformed to their equivalent values in cylindrical specimens. This variable was not recorded in some of the experimental set ups in Table 2.
- Bond length to rebar diameter ratio (*l/d*).
- Concrete cover to rebar diameter ratio (*c/d*).
- Age at testing, expressed in days.
- Ratio between the duration of the thermal saturation plateau and the specimen size squared (δ, in hours/dm^2). Given the range of specimen sizes and the range of times allotted for thermal saturation, this variable is defined in order to ascertain whether this aspect of the methodology affects the results or not.
- Exposure temperature (*T*, in °C).

The dependent variables are:

- Normalised residual bond strength (*NRBS*) expressed as a percentage. This is the ratio between the residual bond strength after high temperature exposure and the original bond strength at ambient temperature.
- The compressive strength after high temperature exposure ($f_{c,T}$, in MPa), whenever the experiments covered this type of test.
- The original peak bond strength value at ambient temperature ($\tau_{b,20\,°C}$, in MPa).

Concerning the experimental data points represented in Fig. 2, only the available results for ribbed deformed steel reinforcing bars have been considered in the database. That means that the experiments reported by Kasami et al. (1975) [24] have not been included because they focused on the bond between concrete and plain round bars. Also, results for plain round bars or prestressing wires reported in [23], [25], [26], [28], [33] have been left out. In the case of the research by Ergün et

al. (2016) [33], these authors studied the effect of the steel grade on the bond behaviour and the database illustrated in Fig. 2 only includes those results that correspond to the usual yield strength of reinforcing bars (around 500 MPa). Finally, in the case of the research by Yang et al. (2018) [37], these authors focused on the effect of slightly corroded rebars on the bond at high temperature and the database only collects the results corresponding to low values of mass-loss (not greater than 1%).

Table 3. Example of database entries

Reference	Fibre type	Fibre VF [%]	$f_{c,20\,°C}$ [MPa]	l/d	c/d	Age [days]	δ [h/dm^2]	T [°C]	$f_{c,T}$ [MPa]	$\tau_{b,20\,°C}$ [MPa]	$NRBS$ [%]
Varona et al. [35] (C)	3	0.41	20.5	4.17	4.71	60	0.8	20	20.5	12.7	100
Varona et al. [35] (C)	3	0.41	20.5	4.17	4.71	60	0.8	450	17.1	12.7	82.68
Varona et al. [35] (C)	3	0.41	20.5	4.17	4.71	60	0.8	650	10.4	12.7	44.80
Varona et al. [35] (C)	3	0.41	20.5	4.17	4.71	60	0.8	825	3	12.7	26.93
Varona et al. [35] (D)	2	0.27	74.2	4.17	4.71	60	0.8	20	74.2	30.1	100
Varona et al. [35] (D)	2	0.27	74.2	4.17	4.71	60	0.8	450	60.4	30.1	90.70
Varona et al. [35] (D)	2	0.27	74.2	4.17	4.71	60	0.8	650	29.9	30.1	33.89
Varona et al. [35] (D)	2	0.27	74.2	4.17	4.71	60	0.8	825	18.1	30.1	16.58

3.2 Additional experimental programme

In order to validate the prediction models of the bond strength at high temperature, this paper presents an additional experimental study. Four concrete batches were prepared: two of them were of normal strength concrete (NSC) and the other two of high strength concrete (HSC). Polypropylene fibre addition was considered for both HSC batches, one of which also included hook-end steel fibres. One of the NSC batches was plain concrete and the other one did include hook-end steel fibres. The concrete compositions are given in Table 4.

Table 4. Compositions of concretes tested in experimental programme

	NSC-1	NSC-2	HSC-1	HSC-2
Cement [kg/m^3]	418	418	450	450
Cement type	CEM II/B-L 32.5R	CEM II/B-L 32.5R	CEM I 52.5R	CEM I 52.5R
Water [kg/m^3]	230	230	173	173
Sand 0/4 [kg/m^3]	694	694	835	835
Limestone gravel 6/12 [kg/m^3]	1042	1042	835	835
Silica fume [kg/m^3]	–	–	45	45
Polypropylene fibres [kg/m^3]	–	–	3	3
Steel fibres [kg/m^3]	–	20	–	20

The polypropylene fibres had a length of 6 mm and a diameter between 31 and 35 μm. The material was 100% polypropylene, with a melting point around 165 °C: The steel fibres were of the hook-end type with a length of 35 mm and a diameter of 0.75 mm.

The specimens were unmoulded at 24 h and then stored until an age of 28 days in a chamber under controlled conditions (20 ± 2 °C and relative humidity over 95%). Some of the samples were tested at room temperature at an age of 28 days and the rest were stored under normal conditions inside the laboratory until an age of 60-62 days. Then, further tests at room temperature were carried out plus the thermal treatments and the tests after high temperature exposure. A total of 120 specimens were thus prepared, half of them for the compressive strength tests and the other half for the pull-out tests. For each test, five different conditions were chosen –age of 28 days at room temperature (T_{amb}) and age of 60 days at T_{amb}, 450, 650 and 825 °C– with three specimens for each condition and concrete batch. The compressive strength tests were carried out on cylindrical specimens with a height of 300 mm and a diameter of 150 mm, in compliance with EN 12390-3 [40]. On the other hand, the bond strength was measured through a modified version of the pull-out test, using a cylindrical specimen with a steel ribbed reinforcement bar embedded along its axis. The bond length was limited to just 50 mm, in accordance with [38]. The test setup is shown in Fig. 3 and the following specimen dimensions were considered:

- 100 mm high cylinders with a diameter of 100 mm in the case of NSC-1 and NSC-2. The steel reinforcement bar had a nominal diameter of 10 mm.
- 130 mm high cylinders with a diameter of 125 mm in the case of HSC-1 and HSC-2. The steel reinforcement bar had a nominal diameter of 12 mm.

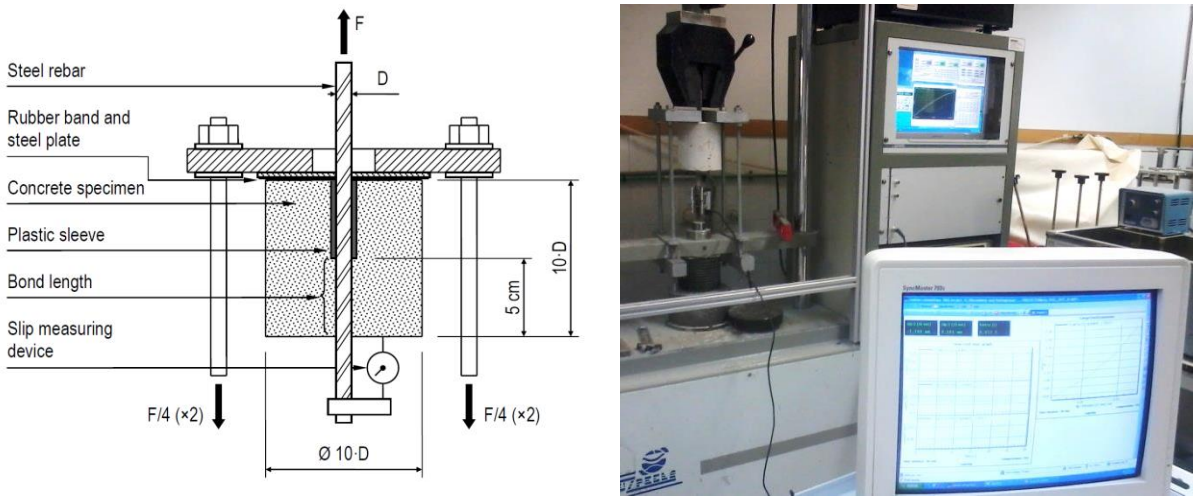

(a) (b)

Fig. 3 Bond strength assessed through pull-out test: (a) schematic setup; (b) instrumentation of the test

The heating rate was 4.5 °C/min and the maximum target temperature was maintained during 75 minutes. Natural cooling took place inside the oven and lasted typically between 11 and 16 hours.

4. Results of the experimental programme

The experimental results are given in Table 5. The structure of the database used to store the results of the studies presented in the literature review section has been used to show this information.

Table 5. Results of the experimental programme

Batch	Fibre type	Fibre VF [%]	$f_{c,20\,°C}$ [MPa]	*l/d*	*c/d*	Age [days]	δ [h/dm^2]	*T* [°C]	$f_{c,T}$ [MPa]	$\sigma_{b,20\,°C}$ [MPa]	*NRBS* [%]
NSC-1	0	0.00	27.3	5.00	4.50	60	1.25	20	27.3	19.1	100
NSC-1	0	0.00	27.3	5.00	4.50	60	1.25	450	21.0	19.1	69.85
NSC-1	0	0.00	27.3	5.00	4.50	61	1.25	650	10.1	19.1	29.34
NSC-1	0	0.00	27.3	5.00	4.50	62	1.25	825	3.9	19.1	10.82
NSC-2	1	0.25	28.1	5.00	4.50	60	1.25	20	28.1	16.7	100
NSC-2	1	0.25	28.1	5.00	4.50	60	1.25	450	21.3	16.7	85.93
NSC-2	1	0.25	28.1	5.00	4.50	61	1.25	650	12.3	16.7	45.83
NSC-2	1	0.25	28.1	5.00	4.50	62	1.25	825	4.6	16.7	13.93
HSC-1	2	0.34	85.1	4.17	4.71	60	0.80	20	85.1	30.6	100
HSC-1	2	0.34	85.1	4.17	4.71	60	0.80	450	61.2	30.6	70.01
HSC-1	2	0.34	85.1	4.17	4.71	61	0.80	650	40.5	30.6	41.58
HSC-1	2	0.34	85.1	4.17	4.71	62	0.80	825	18.4	30.6	12.12
HSC-2	3	0.59	88.7	4.17	4.71	60	0.80	20	88.7	29.8	100
HSC-2	3	0.59	88.7	4.17	4.71	60	0.80	450	70.1	29.8	74.32
HSC-2	3	0.59	88.7	4.17	4.71	61	0.80	650	42.1	29.8	51.80
HSC-2	3	0.59	88.7	4.17	4.71	62	0.80	825	19.3	29.8	14.67

In Tables 3 and 5, the fibre type 0 corresponds to concretes without fibres; fibre type 1 corresponds to steel fibre reinforced concretes; fibre type 2 corresponds to polypropylene fibre reinforced concrete; and fibre type 3 corresponds to hybrid fibre additions, mixing steel and polypropylene. One important result in the experimental programme conducted here is that there were no spalling failures, not even in the HSC samples with compressive strength over 80 MPa and in spite of the high temperatures tested –equal or in excess of 650 °C. Also, no sloughing off was observed in the surface of the specimens. According to Eurocode 2, Part 1-2 [22], when HSC is prepared using a significant amount of silica fume (over 6% by weight of cement), a minimum of 2 kg/m^3 of monofilament polypropylene fibre (PPF) is recommended in the concrete mix. In this case, the content of silica fume was 10% by cement weight and, as shown in Table 4, the amount of PPF was 3 kg/m^3, which may explain the good behaviour exhibited by the HSC batches: the melting of PPF at around 170 °C creates a capillary network that helps reducing the vapour pressure build-up associated

to the dehydration reactions of the cement paste components. This finding is also in accordance with previous experimental observations reported by [15]–[18].

5. Multiple variable regression analyses

The use of databases collecting previously reported empirical results to develop prediction models has already been successfully applied to mechanical properties of concrete exposed to high temperatures [19], [20]. In this particular case, the information contained in the database which has been presented earlier in this paper could be used to develop a non-linear simple regression analysis for the normalised residual bond strength (*NRBS*) with the exposure temperature as the only independent variable (see Fig. 2), which would yield Eq. [12]:

$$NRBS = A_0 + B_0 \cdot T + C_0 \cdot T^2 \qquad [12]$$

where *NRBS* is the normalised residual bond strength (in %), T is the maximum exposure temperature (in °C), A_0 = 102.8 ± 2.6, B_0 = -0.0726 ± 0.0165 and C_0 = (-4.07 ± 2.11)·10^{-5}. Coefficients A_0, B_0 and C_0 are expressed by an estimated value plus or minus a margin for the 95% confidence interval. The R^2 coefficient for this regression analysis is 0.802. The mean estimation curve and its 95% confidence interval are represented in Fig. 2. The wide dispersion at the highest range of temperatures may be explained by the attempt to predict *NRBS* as a function of just one variable.

The eight independent variables in Table 3 are now considered for a linear multiple analysis. The dependent variable is the normalised residual bond strength (*NRBS*). Before carrying out this analysis, the database was slightly truncated because some of the experiments ([11], [23], [25]–[27], [36]) did not record the value of the compressive strength at ambient temperature. Next, a few outlier results were removed. One of them is easily appreciated in Fig. 2: at a temperature of 300 °C one experiment predicted a *NRBS* of around 20%. The results from that test –not only at 300 °C but also at other temperatures– were withdrawn. Other outliers were identified at 800 °C predicting a *NRBS* equal to 0. These adjustments reduced the number of data points from 450 to 372. When carrying out multiple regression analyses it is usually recommended that the number of data points per independent variable be at least 20 to 50. Considering eight variables (fibre type, fibre volume fraction, compressive strength at ambient temperature $f_{c,20\,°C}$, ratio l/d, ratio c/d, age at testing, ratio δ of thermal saturation plateau to specimen size squared, and temperature T), the database would yield 46 points per independent variable, which seems adequate.

The linear multiple regression analysis was carried out with SPSS software. A backward elimination method was selected to check the possibility of reducing the number of independent variables. The most important statistical parameters are shown in Table 4. Three models were created and studied. The first one (Model 1) included all eight independent variables. The second one (Model 2) removed one independent variable and the third one (Model 3) removed another one, leaving a

total of six independent variables. The criterion used to remove variables was based on the contribution of each variable to the regression equation: a predictor variable was removed when its statistical significance was equal or greater than 8%. The greatest significance value of the independent variables in Model 3 was 2.1%, so the linear multiple regression analysis may be explained with just six predictor variables.

Table 6. Linear multiple regression models

	R^2	Adjusted R^2	Durbin-Watson	ANOVA test		Condition index	Removed variables	VIF of removed variables
				F	sig.			
Model 1	0.830	0.826	1.489	220.8	< 0.0001	29.48	None	–
Model 2	0.829	0.826	1.488	252.1	< 0.0001	23.69	δ	6.519
Model 3	0.828	0.825	1.476	292.0	< 0.0001	16.55	δ $f_{c,20\ ^\circ C}$	5.892 2.227

Therefore, from a statistical point of view, neither the ratio δ nor the original concrete compressive strength at ambient temperature $f_{c,20\ ^\circ C}$ seem to have a significant impact on the loss of bond strength at high temperature. This would mean that despite the relatively great disparity between the durations of the thermal saturation treatments and also between the sizes of the pull-out specimens in the sources of the database, this feature may not be statistically significant in the prediction model.

Once that the relevant variables had been identified, a new multiple regression analysis was carried out, defining a non-linear quadratic dependence for the temperature *T* and linear functions for the other five variables: fibre type (*FT*), fibre volume fraction (*VF*, expressed as percentage), bond length to bar diameter (*l/d*), concrete cover to bar diameter (*c/t*) and age at testing (*Age*). The result is shown in Eq. [13].

$$NRBS = A_1 + B_1 \cdot T + C_1 \cdot T^2 + D_1 \cdot FT + E_1 \cdot VF + F_1 \cdot \frac{l}{d} + G_1 \cdot \frac{c}{d} + H_1 \cdot Age \qquad [13]$$

where A_1 = 109.3 ± 6.6, B_1 = -0.0715 ± 0.0161, C_1 = (-3.51 ± 2.11)·10^{-5}, D_1 = 3.33 ± 2.02, E_1 = -7.34 ± 4.12, F_1 = 0.674 ± 0.229, G_1 = -2.41 ± 1.22 and H_1 = -0.0514 ± 0.0537. As before, these coefficients are expressed with an estimated mean value plus or minus a margin for the 95% confidence interval. The R^2 coefficient for this regression analysis is 0.833, which does not seem a significant improvement over the linear multiple regression analysis based on the exposure temperature as the only predictor variable (R^2 = 0.802). The model could be then described through the four-variable Eq. [14], valid for plain concrete (i.e., without fibre addition):

$$NRBS_{plain\ concrete} = 109.3 - 0.0715\,T - 3.51 \cdot 10^{-5} T^2 + 0.674 \frac{l}{d} - 2.41 \frac{c}{d} - 0.0514\,Age \qquad [14]$$

where T is the exposure temperature (in °C), d is the ribbed bar diameter, l is the bond length, c is the concrete cover and *Age* is expressed in days. The generalisation for fibre reinforced concrete (FRC) is presented in Eq. [15]:

$$NRBS_{FRC} = NRBS_{plain\ concrete} + 3.33\,t_f - 7.34\,v_f \qquad [15]$$

where t_f is the type of fibre (1 for steel fibre, 2 for polypropylene fibre and 3 for hybrid fibre addition) and v_f is the fibre content (as volumetric percentage).

The application of Eq. [14] to plain concretes is illustrated in Fig. 4a and Fig. 4b. The former corresponds to a situation at an age of 28 days, with l/d = 5 and c/d = 5. The mean prediction curve for this case and its upper and lower limits are represented in Fig. 4a which also shows the experimental database results that comply with those features. A second example is shown in Fig. 4b, which also corresponds to plain concrete, but at an age of 40 days, with l/d = 8 and c/d = 2. The experimental data points given in Fig. 4b roughly match these values: age between 35 and 40 days, l/d between 7.5 and 8.3, and c/d between 1.78 and 2.28.

The multiple variable model seems capable enough of adapting to different situations but unfortunately its confidence interval is notoriously wider than that of the one-variable non-linear model described by Eq. [12] and represented in Fig. 2. For example, the lower limit of the single-variable model would predict a complete loss of the NRBS at a temperature around 750 °C, regardless of other factors (age, fibre content, bond length and concrete cover), whilst the model itself –its mean curve– would have a NRBS of 25.7% at 750 °C. In the case of plain concrete at 28 days, with l/d = c/d = 5, the lower limit of the multiple variable model shows a total loss of NRBS at around 675 °C but the model would predict a NRBS of 34.9% because the confidence interval has spread.

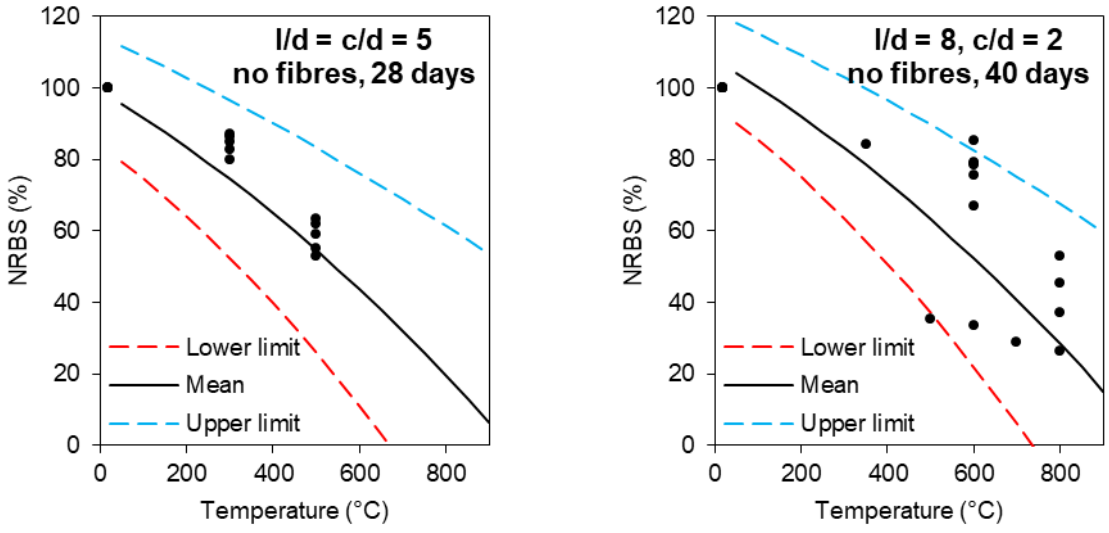

(a) (b)

Fig. 4 Application of the non-linear multiple regression model for bond strength as a function of six variables.

The single variable model (SVM) of Eq. [12] and the general multiple variable model (MVM) of Eq. [13] are now compared with some of the analytical models presented in this paper's literature review section (Eq. [1] to Eq. [11]). All models are tested under the experimental input parameters available in the database and their predicted results are contrasted with the experimental evidence collected in the database. Most models in the literature review section are based on plain concrete, i.e., concrete without fibre addition. Moreover, the model by Aslani and Samali [39] is the only one which had been based on a wide array of previously reported results, none of which corresponded to FRC. Therefore, the database for the model comparison only includes plain concrete sources (either normal strength concrete or high strength concrete) or concretes with a small amount of monofilament polypropylene fibres (t_f = 2) used for explosive spalling control. Also, some of the models depend on the evolution of the compressive strength at high temperature, so the database only includes those references which also reported this feature. Finally, the analytical model by Arel and Yazici [32] –Eq. [6]– cannot be compared because it is limited to 14-mm-diameter deformed steel bars and, more importantly, because it depends on some concrete properties –splitting tensile strength and modulus of elasticity– that are not available in most of the experimental setups collected in the database. The following error parameters are used in this discussion: the mean absolute error (*MAE*, Eq. [16]), the mean absolute percentage error (*MAPE*, Eq. [17]) and the root mean square error (*RMSE*, Eq. [18]). These error measurements depend on the experimentally tested values of the dependent variable (R_i), the predicted values of the dependent variables (P_i) and the number of data points used in the comparison (N). The error measurements obtained through the application of the discussed prediction models to the experimental results reported in the state of the art and the additional results in the experimental programme reported in Table 5 are shown in Table 7.

$$MAE = \frac{\sum_{i=1}^{N} |R_i - P_i|}{N} \quad [16]$$

$$MAPE = \frac{\sum_{i=1}^{N} \frac{|R_i - P_i|}{R_i}}{N} \quad [17]$$

$$RMSE = \sqrt{\frac{\sum_{i=1}^{N} (R_i - P_i)^2}{N}} \quad [18]$$

There are some remarks worth mentioning concerning the application of some analytical models from Table 1 into Table 7. In the case of the two models by Aslani and Samali [39], the equations that correspond to the full range of the bond length (30 mm $\leq l \leq$ 160 mm) have been used. In the case of the model by Yang et al. [37] the value of coefficient β is 3.5 for $T \leq$ 400 °C and 2.5 for $T \geq$ 600 °C. For intermediate temperatures in the range from 400 to 600 °C, it is assumed that the β may be

obtained through linear interpolation. Finally, when the models depend on the evolution of the compressive strength ($f_{c,T}$ or *NRCS*), their application uses the experimental values of $f_{c,T}$ available in the database, instead of the accompanying analytical equations provided by their authors.

Table 7. Error measurements of *NRBS* models

Model	Applied to results in state of the art database			Applied to additional experiments in Table 5		
	MAE	***MAPE***	***RMSE***	***MAE***	***MAPE***	***RMSE***
Haddad and Shannis [29], Eq. [1]	18.0	29.6%	21.8	13.2	36.0%	14.7
Haddad et al. [30], Eq. [2]	36.5	53.5%	39.7	28.3	52.5%	34.4
Aslani and Samali [39], Eq. [3]-[4]	9.5	19.3%	13.0	9.8	31.3%	12.2
Aslani and Samali [39], Eq. [5]	9.2	21.0%	12.3	10.3	50.8%	12.6
Ergün et al. [33], Eq. [7]-[8]	11.1	20.9%	13.6	9.0	23.0%	10.3
Varona et al. [35], Eq. [9]-[10]	47.9	65.2%	85.8	16.5	28.3%	20.3
Yang et al. [37], Eq. [11]	112	161.7%	153	24.7	78.3%	25.5
Single variable model, Eq. [12]	8.5	17.4%	11.6	6.3	14.5%	8.8
Multiple variable model, Eq. [13]	8.2	16.8%	10.9	6.6	18.9%	8.8

Table 7 presents two sets of error measurements. The first one corresponds to the comparison between the results collected in the state of the art's database –329 experiments– and the *NRBS* predictions given by each of the analytical models used. Judging from the error measurements given in Table 7, the most accurate model seems to be the general MVM developed in this work (Eq. [13]). Of the previously reported models, the best one is the second set of equations by Aslani and Samali [39] (Eq. [5]) which exhibits a *RMSE* of 12.3 that is greater than the *RMSE* of the MVM (10.9). By far the most inaccurate performance is found in the models by Varona et al. [35] and by Yang et al. [37] and the reason seems to be that these two models are not designed to predict the normalised residual bond strength but the absolute value of the residual bond strength. Moreover, in both cases the equations make the peak bond strength at high temperature ($\tau_{b,max,T}$) depend on the evolution of the cube compressive strength at high temperature ($f_{c,cub,T}$) for which the real tested values have here been employed instead of the sets of equations originally provided in [35], [37]. The relationship between these two properties –bond strength and compressive strength– is addressed in the next section.

The second set of error measurements in Table 7 compare the analytical models in Eq. [1]-[5] and Eq. [7]-[13] with the experimental results obtained in the additional study presented in this paper, which was summarised in Table 5. The additional study includes plain concrete (the batch NSC-1) and fibre reinforced concretes (batches NSC-2, HSC-1 and HSC-2). Both the SVM and the MVM

developed here are the only models able to reduce the *MAPE* under 20% and the *RMSE* under 10. Therefore, these new prediction models are deemed to offer the most accurate prediction of the additional experimental study presented here, despite their being developed independently of it.

An analysis of the error measurements given in Table 7 shows that there seems to be a very slight advantage of the multi-variable approach over the single-variable one. When confronting these new prediction models with all the experimental background reported in the state of the art, the MVM reduces the *MAPE* in more than 0.5% with respect to the SVM, and the *RMSE* is reduced by 6% (11.6 to 10.9). Furthermore, the MVM would be able to qualitatively explain how some parameters would affect the loss of steel-to-concrete bond at high temperature. For example, the loss of bond with heat exposure is explained with the two negative coefficients for T and T^2 (see Eq. [14]). The concrete cover (c/d) also has a negative coefficient; at first hand, this result is paradoxical, because the thinner the concrete cover, the greater the risk of brittle failure due to concrete splitting instead of pull-out of reinforcing bar. However, the dependent variable in this model is not the absolute value of the bond strength at high temperature ($\tau_{b,T}$) but its normalised value *NRBS* with respect to the original one at ambient temperature ($\tau_{b,20\,°C}$), which is severely compromised if splitting occurs before pulling-out. At high temperatures, the risk of splitting is slightly reduced because the micro-structure's stiffness has been reduced. Therefore, with a thicker concrete cover c, the *NRBS* would compare the bond strength at high temperature ($\tau_{b,T}$) with a greater value of $\tau_{b,20\,°C}$, thus yielding a smaller residual bond strength. Apparently, the age at testing also has a negative impact on *NRBS*, which may be attributed to the fact that in an older concrete, the hydration of the cement paste is higher. Consequently, the mechanical properties at ambient temperature are increased but, at the same time, the cement paste may suffer more damage caused by the dehydration reactions taking place when exposed to elevated temperature. For example, a reinforced concrete element that reached 600 °C –with $l/d = c/d = 5$– would suffer a loss in the residual bond strength between 56% (age of 28 days) and 60% (age of 90 days). At a higher temperature of 800 °C, the loss in residual bond strength would be between 80% (28 days) and 84% (90 days). However, the addition 0.5% in volume of hybrid fibres would reduce the loss in residual bond strength to from 84% to 77% at 800 °C (age of 90 days). A similar result may be observed using polypropylene fibre addition of 0.2% (around 2 kg/m^3), with a bond strength loss of 78% at 800 °C (age of 90 days).

6. Relationship between bond strength and compressive strength

As stated before, the database that has been created using the experimental evidence from the literature review not only includes the *NRBS* values but also the evolution of the compressive strength ($f_{c,T}$) after high temperature exposure and the peak bond strength at ambient temperature ($\tau_{b,20\,°C}$). These data may help studying a possible analytical relationship between the loss of residual bond strength and the loss of compressive strength after exposure of the concrete to elevated temperatures.

Not all the authors referenced in Table 2 reported the evolution of $f_{c,T}$ and, unfortunately, the evidence collected by Milovanov and Salmanov [23], Reichel (1978) [25], Diederichs and Schneider [26], Hertz (1982) [27], Ahmed et al. (1992) [11] and Lee et al. (2018) [36] cannot be used for that purpose. In the dabase there are a total of 381 data points that include $f_{c,T}$ (along with $\tau_{b,20\,°C}$ and *NRBS*). The relationship between the experimental results for $\tau_{b,T}$ and $f_{c,T}$ is illustrated in Fig. 5a. Furthermore, the Model Code 2010 [21] suggests a linear relationship between the bond strength and the square root of the compressive strength and this feature is shown in Fig. 5b.

The poor values of the R^2 coefficients in the linear regression analyses represented in Fig 5a and Fig. 5b may be explained by the wide range of values of ratios *c/d* (cover to bar diameter) and *l/d* (bond length to bar diameter). According to the Model Code 2010, the bond stress-slip local relationship strongly depends on these ratios. For example, low values of *c/d* –smaller than 5– may induce splitting failure to occur before pull-out failure. The former is likely to produce low values of the peak bond strength. Concerning the *l/d* ratio, the pull-out set up should be limited to a bond length not greater than five times the bar diameter in order for the experiment to yield an experimental bond stress-slip relationship that could arguably be taken as the local relationship from the Model Code 2010 (see Fig. 1).

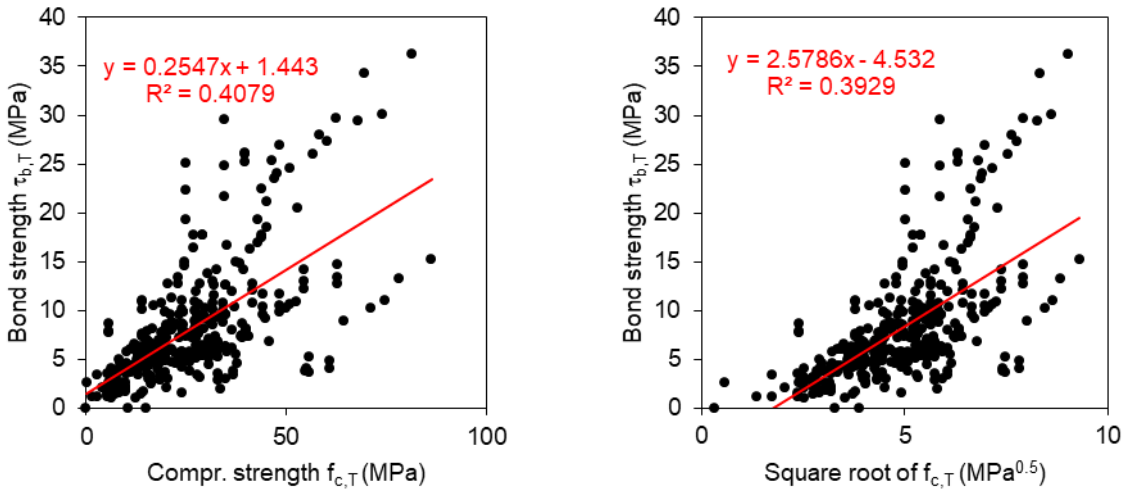

(a) (b)

Fig. 5 Bond strength as a function of (a) the compressive strength and (b) its square root (b): 381 experimental data points and linear regression analyses.

The effect of ratios *c/d* and *l/d* is illustrated through Fig. 6a and Fig. 6b, which represent experimental evidence from tests with $c/d > 3.5$ and $l/d \leq 7.5$ (146 data points, the outlier points removed in the previous section having also been removed here) which roughly exhibit the conditions compatible with the local bond stress-slip curve of Model Code 2010. These 146 data are presented in series 'SoA' (it stands for state of the art). The dispersion has been reduced and the linear regression

curves exhibit better values of the R^2 coefficients. Furthermore, the 16 additional empirical results obtained in the experimental study reported in this paper are also represented in in Fig. 6a and 6b, through series 'Exp.', which fit into the range $c/d > 3.5$ and $l/d \leq 7.5$.

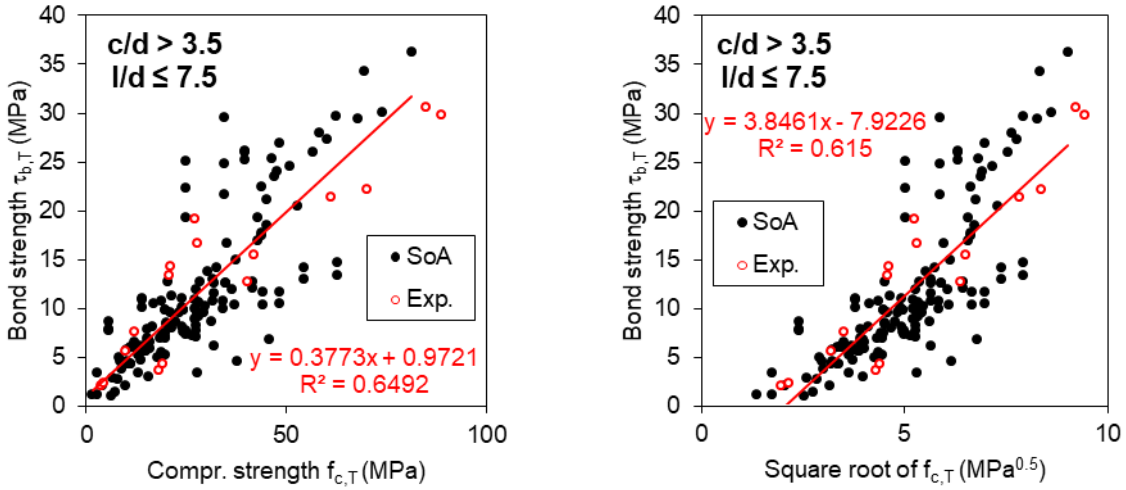

(a) (b)

Fig. 6 Bond strength as a function of (a) the compressive strength and (b) its square root (b): 'SoA' series is sourced from the state of the art's experiments with $c/d > 3.5$ and $l/d \leq 7.5$; 'Exp.' series presents the 16 experimental results reported in this paper.

A nonlinear multiple regression analysis was performed to try to predict the peak bond strength after high temperature exposure with an equation similar to that one in Model Code 2010. This model is described by Eq. [19]:

$$\tau_{b,max,T} = k_b \cdot \left(f_{c,T} \right)^n \qquad [19]$$

where k_b is a coefficient that accounts for the quality of the bond conditions, which might be affected by high temperature exposure –equivalent to coefficient β in the model by Yang et al. [37]. The regression analysis would try to obtain the relationship between coefficient k_b and a number of variables: the exposure temperature (T), the type of fibre (FT), the fibre volume fraction (VF), the l/d ratio, the c/d ratio and the age at testing (Age). This relationship is illustrated in Eq. [20]:

$$k_b = A_3 + B_3 \cdot T + C_3 \cdot FT + D_3 \cdot VF + E_3 \cdot \frac{l}{d} + F_3 \cdot \frac{c}{d} + G_3 \cdot Age \qquad [20]$$

Given that the number of independent variables is 6 and the number of available data points is 142, there are around 24 points per variable, which lies within the recommended range. Three non-linear regression analyses were thus performed: (i) with the power n equal to 0.5 (according to Fig. 6b); (ii) with the power n equal to 1 (Fig. 6a); and (iii) with the power n as an unknown coefficient to be obtained through regression, similarly to coefficients A_3 through G_3. The results are shown in Table 8.

503 The single variable models for the relationships between $\tau_{b,max,T}$ and $\left(f_{c,T}\right)^n$ are illustrated in Fig.
504 6a and Fig. 6b, with $f_{c,T}$ or $\sqrt{f_{c,T}}$ as the only independent variable (x). These regression lines
505 exhibited R^2 values of 0.649 (with n = 1, Fig. 6a) and 0.615 (with n = 0.5, Fig. 6b). However, the
506 multiple variable based models given by Eq. [19]-[20], which are shown in Table 8, outdo the former
507 models with values of R^2 over 0.8. This fact seems to demonstrate that the multiple variable approach
508 is entirely suitable for explaining the evolution of the bond strength at high temperature by means of a
509 generalised form of the peak bond strength equation of Model Code 2010. Moreover, the most
510 striking finding of this work is that when the value of the power n is subjected to the non-linear
511 regression analysis, the result (n = 0.639) is very close to the value suggested in the Model Code 2010
512 (n = 0.5), even though the value n = 1 had initially yielded a better R^2 coefficient in the single
513 variable approach.
514
515 Table 8. Results of regression analyses for $\tau_{b,max,T}$ given by Eq. [19]-[20]

	Power n = 0.5	**Power n = 1**	**Power n = 0.639 ± 0.100**
A_3	0.854 ± 0.886	-(0.0860 ± 0.1674)	0.268 ± 0.589
B_3	-(0.00209 ± 0.00039)	$-(1.05 \pm 0.77)\cdot 10^{-4}$	-(0.00101 ± 0.00059)
C_3	-(0.309 ± 0.171)	-(0.0578 ± 0.0299)	-(0.187 ± 0.116)
D_3	1.90 ± 0.89	0.115 ± 0.148	0.904 ± 0.707
E_3	-(0.348 ± 0.091)	-(0.0595 ± 0.0165)	-(0.211 ± 0.094)
F_3	0.550 ± 0.246	0.129 ± 0.045	0.370 ± 0.181
G_3	0.0306 ± 0.0089	0.00529 ± 0.00156	0.0194 ± 0.0082
R^2 factor	0.871	0.837	0.879

516
517 Furthermore, it is possible to give a physical explanation for the model represented through Eq.
518 [19]-[20]. The peak bond strength at temperature T would not only be reduced as a consequence of
519 the loss of concrete compressive strength $f_{c,T}$ but also because high temperature damages the quality
520 of the bond condition associated with coefficient k_b. The signs of coefficients A_3 through G_3 represent
521 the effect of the variables on the bond condition: positive (> 0) or negative (< 0). Temperature, type
522 of fibre and bond length seem to have a negative impact on the bond quality. Conversely, fibre
523 volume fraction, concrete cover and age at testing would have positive effect. In summary, the peak
524 bond strength after high temperature exposure $\tau_{b,max,T}$ (in MPa) may be described through Eq. [21]:

525 $$\tau_{b,max,T} = k_b \cdot \left(f_{c,T}\right)^{0.639} \qquad [21]$$

526 where $f_{c,T}$ is the concrete compressive strength (in MPa) at temperature T (in °C) and coefficient
527 k_b is calculated though Eq. [22] for plain concrete (without fibre addition):

528 $$k_b = k_{b,\,plain\ concrete} = 0.268 - 0.00101T - 0.211\frac{l}{d} + 0.370\frac{c}{d} + 0.0194\,Age \qquad [22]$$

where l is the bond length, d is the ribbed bar diameter, c is the clear concrete cover of the bar and the *Age* is expressed in days. In the case of fibre reinforced concretes, coefficient k_b is given by Eq. [23]:

$$k_b = k_{b,\,plain\ concrete} - 0.187\,FT + 0.904\,VF \qquad [23]$$

where *FT* is the type of fibre –defined earlier in the paper– and *VF* is the fibre volume fraction expressed as a percentage.

The application of this model at room temperature (20 °C) would predict a value of k_b = 1.59 (age of 28 days) or k_b = 2.79 (age of 90 days) for a reinforced concrete without fibre addition and $l/d = c/d$ = 5. These results show reasonable agreement with the values recommended in the Model Code 2010 (between 1.25 and 2.5, depending on the bond condition). Based on Eq. [22], in a reinforced concrete element exposed at 800 °C, coefficient k_b would suffer a loss between 28% (age of 90 days) and 50% (age of 28 days). The effect of fibres seems to have positive effect on the bond condition at high temperature. For instance, a 90 days reinforced concrete at 800 °C would exhibit a k_b = 2.00; the addition of a 0.5% of steel fibres might increase k_b by a 13%, whereas hybrid fibre addition (0.5% of steel fibres plus 0.2% of polypropylene fibres) might increase k_b by a 3.6% with respect to the plain concrete.

As stated in the previous section, the analytical models by Varona et al. [35] and Yang et al. [37] attempted to predict the peak bond strength at high temperature ($\tau_{b,max,T}$) instead of aiming at the normalised residual (peak) bond strength (*NRBS*), which was the objective of the rest of the models collected in Table 2. The model by Yang et al. was based on the equation of the Model Code 2010 with n = 0.5, whilst Varona et al. devised a linear relationship (n = 1) between $\tau_{b,maxT}$ and $f_{c,T}$. The database with the 146 state of the art's experiments that correspond to test conditions close to Model Code 2010 is now used to compare these two models with the multiple variable model of the Model Code 2010 equation (MVM-MC) given by Eq. [21]-[23]. The error measurements observed in the predictions are annotated in Table 9. The MVM-MC developed in this work is the model that best fits the available experimental results (*MAPE* = 22.6%, *RMSE* = 2.65).

Table 9. Error measurements of $\tau_{b,max,T}$ models

	Applied to results in state of the art database			**Applied to additional experiments in Table 5**		
Model	***MAE***	***MAPE***	***RMSE***	***MAE***	***MAPE***	***RMSE***
Varona et al. [35], Eq. [9]-[10]	3.01	30.2%	4.42	3.79	28.3%	4.61
Yang et al. [37], Eq. [11]	7.04	97.3%	8.09	4.34	62.7%	4.86
MVM-MC, Eq. [21]-[23]	1.96	22.6%	2.65	3.24	34.0%	4.10

A second set of error measurements is included in Table 9, to compare the additional results from the experimental programme reported in Table 5 with the $\tau_{b,T}$ values that would be estimated through

Eq. [9]-[11] and Eq. [21]-[23]. In this case the *MAPE* error favours the model by Varona et al. [35] whilst the new multi-variable generalisation of the Model Code 2010 formulation developed in this paper exhibits the minimum *RMSE*.

6. Conclusions

The evolution of the bond between reinforcing steel and concrete at elevated temperatures is not addressed by structural concrete standards and, moreover, is one of the least researched topics in concrete technology. This paper attempts to present a thorough literature review of experimental studies that have been reported since the 1950's, which have been systematically collected in a database of experimental results. The disparity between the test conditions has been taken into account through the identification of eleven variables: exposure temperature, concrete compressive strength at ambient temperature, type of fibre, fibre volume fraction, ratio of bond length to bar diameter, ratio of concrete cover to bar diameter, ratio of thermal saturation plateau to specimen size squared, age at testing, normalised residual bond strength, concrete compressive strength at high temperature and peak bond strength at ambient temperature. All the experimental setups used modified versions of the pull-out test and the geometry of the specimen was cylindrical in most cases. However, few tests tried to reproduce the conditions of the local bond stress-slip relationship of the Model Code 2010 [21] in terms of bond length and sufficient clear concrete cover, despite of what, some authors tried to adapt the formulation for the peak bond strength in the Model Code 2010 for high temperature exposure.

Based on the experimental results available, two regression analyses have been devised. The first is aimed at predicting the normalised residual bond strength as a function of the exposure temperature and five more independent variables. Using the experimental results available in the database as a source, this model compares favourably with previous analytical models. Furthermore, this multi-variable approach describes the impact that relevant variables have on the bond behaviour at high temperature:

- The clear concrete cover has a negative effect on the normalised residual bond strength because thinner covers may cause a premature brittle failure at ambient temperature and thus reduce the original value to which is compared the bond strength at high temperature, which is less likely to fail by splitting.
- The age at testing also has a negative impact on the normalised residual bond strength. For example, at 800 °C the loss in bond strength in a 90 days old reinforced concrete element would be increased by 16% with respect to a 28 days old sample. This may be attributed to the fact that the hydration of the cement paste is higher in older concretes. Consequently, the mechanical properties at ambient temperature are increased but, at the same time, the cement paste may suffer more damage caused by the dehydration reactions taking place when exposed to elevated temperature.

- The addition of fibres seems to have a beneficial impact on the bond strength at high temperature. The model predicts that the addition of 0.5% in volume of hybrid fibres would reduce the loss in residual bond strength by 7.6% at 800 °C. A similar effect might be obtained with the addition of 0.2% of polypropylene fibres.
- From a statistical point of view, the compressive strength at room temperature would not have a significant effect on the evolution of the bond strength after high temperature exposure.

A second multi-variable non-linear regression analysis succeeds in adapting the Model Code 2010's equation to predict the peak bond strength after high temperature exposure. This equation defines a relationship between the peak bond strength at a given temperature and the concrete compressive strength (at the same temperature) to the power n. The optimum value of n was found to be 0.639 and is fairly close to the original value in the Model Code 2010. The equation includes a coefficient k_b associated with the quality of the bond condition, which depends on the exposure temperature and five more independent variables. At room temperature the value of k_b ranges 1.59 to 2.79 depending on the age of the reinforced concrete element (28 to 90 days), which reasonably agrees with the recommended values in the Model Code 2010. This coefficient could be reduced by 30-50% at 800 °C in some cases, which demonstrates that the bond strength after exposure to elevated temperature is compromised not only because of the loss of concrete compressive strength but also because high temperature exposure damages the quality of the bond condition between concrete and steel. A negative linear relationship has been found between high temperature exposure and bond condition, whereas the concrete maturation, the clear cover of the ribbed bar and the fibre content have been found to have a positive effect on the bond condition. For example, the addition of 0.5% of steel fibres may enhance the bond condition by a 13% after exposure to 800 °C.

This paper also reports the results of an additional experimental study that has been carried out and is focused on the evolution of the concrete compressive strength and the bond strength after high temperature exposure. The experimental programme included normal strength and high strength concretes without or with fibre content. These additional experimental results have been used to compare the previous prediction models available in the state of the art with the new models developed in this paper for the normalised residual bond strength and the peak bond strength at high temperature, which have been thus validated.

Acknowledgements

The authors want to acknowledge Generalitat Valenciana, which has made possible this piece of research through the grant GV/2018/015.

References

[1] F. C. Lea, “The effect of temperature on some of the properties of materials,” *Eng.*, vol. 110, no. 3, pp. 293–298, 1920.

[2] Z. P. Bazant and M. F. Kaplan, *Concrete at High Temperatures: Material Properties and Mathematical Models*. Harlow, Essex: Longman Group, Ltd., 1996.

[3] Y. Anderberg and S. Thelandersson, “Stress and deformation characteristics of concrete at high temperatures - 2. Experimental investigation and material behaviour model,” *Bull. Lund Inst. Technol.*, no. 54, pp. 1–84, 1976.

[4] C. Castillo and A. J. Durrani, “Effect of transient high temperature on high strength concrete,” *ACI Mater. J.*, vol. 87, no. 1, pp. 47–53, 1987.

[5] V. Kodur, “Fire performance of high-strength concrete structural members,” *Constr. Technol. Updat.*, p. 4, 1999.

[6] B. Persson, “Fire resistance of self-compacting concrete, SCC,” *Mater. Struct.*, vol. 37, no. 9, pp. 575–584, Nov. 2004.

[7] K. K. Sideris, “Mechanical characteristics of self-consolidating concretes exposed to elevated temperatures,” *J. Mater. Civ. Eng.*, vol. 19, no. 8, pp. 648–654, Aug. 2007.

[8] N. Anagnostopoulos, K. K. Sideris, and A. Georgiadis, “Mechanical characteristics of self-compacting concretes with different filler materials, exposed to elevated temperatures,” *Mater. Struct.*, vol. 42, no. 10, pp. 1393–1405, Dec. 2009.

[9] D. Foti, “Prestressed slab beams subjected to high temperatures,” *Compos. Part B Eng.*, vol. 58, pp. 242–250, 2014.

[10] C. G. Bailey and E. Ellobody, “Whole-building behaviour of bonded post-tensioned concrete floor plates exposed to fire,” *Eng. Struct.*, vol. 31, no. 8, pp. 1800–1810, Aug. 2009.

[11] A. E. Ahmed, A. H. Al-Shaikh, and T. I. Arafat, “Residual compressive and bond strengths of limestone aggregate concrete subjected to elevated temperatures,” *Mag. Concr. Res.*, vol. 44, no. 159, pp. 117–125, 1992.

[12] F. P. Cheng, V. K. R. Kodur, and T. C. Wang, “Stress-strain curves for high strength concrete at elevated temperatures,” *J. Mater. Civ. Eng.*, vol. 16, no. 1, pp. 84–90, 2004.

[13] C. S. Poon, Z. H. Shui, and L. Lam, “Compressive behavior of fiber reinforced high-performance concrete subjected to elevated temperatures,” *Cem. Concr. Res.*, vol. 34, no. 12, pp. 2215–2222, 2004.

[14] A. Lau and M. Anson, “Effect of high temperatures on high performance steel fibre reinforced concrete,” *Cem. Concr. Res.*, vol. 36, no. 9, pp. 1698–1707, 2006.

[15] G. F. Peng, W. W. Yang, J. Zhao, Y. F. Liu, S. H. Bian, and L. H. Zhao, “Explosive spalling and residual mechanical properties of fiber-toughened high-performance concrete subjected to high temperatures,” *Cem. Concr. Res.*, vol. 36, no. 4, pp. 723–727, 2006.

[16] G. F. Peng, S. H. Bian, Z. Q. Guo, J. Zhao, X. L. Peng, and Y. C. Jiang, “Effect of thermal shock due to rapid cooling on residual mechanical properties of fiber concrete exposed to high

temperatures," *Constr. Build. Mater.*, vol. 22, no. 5, pp. 948–955, 2008.

[17] Y. Ding, C. Azevedo, J. B. Aguiar, and S. Jalali, "Study on residual behaviour and flexural toughness of fibre cocktail reinforced self compacting high performance concrete after exposure to high temperature," *Constr. Build. Mater.*, vol. 26, no. 1, pp. 21–31, 2012.

[18] F. B. Varona, F. J. Baeza, D. Bru, and S. Ivorra, "Influence of high temperature on the mechanical properties of hybrid fibre reinforced normal and high strength concrete," *Constr. Build. Mater.*, vol. 159, pp. 73–82, 2018.

[19] F. Aslani and B. Samali, "High strength polypropylene fibre reinforcement concrete at high temperature," *Fire Technol.*, vol. 50, no. 5, pp. 1229–1247, Sep. 2014.

[20] F. Aslani and B. Samali, "Constitutive relationships for steel fibre reinforced concrete at elevated temperatures," *Fire Technol.*, vol. 50, no. 5, pp. 1249–1268, 2014.

[21] International Federation for Structural Concrete (fib), *fib Model Code for Concrete Structures 2010*. Berlin: Ernst & Sohn, 2013.

[22] European Committee for Standarisation, *Eurocode 2: Design of concrete structures - Part 1-2: General rules - Structural fire design*. Madrid: AENOR, 2011.

[23] A. F. Milovanov and G. D. Salmanov, "The influence of high temperatures upon the properties of reinforcing steels and bond strength between reinforcement and concrete," *Issled. po Zharoupornym Betonu i Zhelezobetonu*, pp. 203–223, 1954.

[24] H. Kasami, T. Okuno, and S. Yamane, "Properties of concrete exposed to sustained elevated temperature," in *Transactions of the 3rd International Conference on Structural Mechanics in Reactor Technology, London*, 1975, p. H1/5.

[25] V. Reichel, "How fire affects steel-to-concrete bond," *Build. Res. Pract.*, vol. 6, no. 3, pp. 176–187, 1978.

[26] U. Diederichs and U. Schneider, "Bond strength at high temperatures," *Mag. Concr. Res.*, vol. 33, no. 115, pp. 75–84, 1981.

[27] K. Hertz, "The anchorage capacity of reinforcing bars at normal and high temperatures," *Mag. Concr. Res.*, vol. 34, no. 121, pp. 213–220, 1982.

[28] P. D. Morley and R. Royles, "Response of the bond in reinforced concrete to high temperatures," *Mag. Concr. Res.*, vol. 35, no. 123, pp. 67–74, 1983.

[29] R. H. Haddad and L. G. Shannis, "Post-fire behavior of bond between high strength pozzolanic concrete and reinforcing steel," *Constr. Build. Mater.*, vol. 18, no. 6, pp. 425–435, 2004.

[30] R. H. Haddad, R. J. Al-Saleh, and N. M. Al-Akhras, "Effect of elevated temperature on bond between steel reinforcement and fiber reinforced concrete," *Fire Saf. J.*, vol. 43, no. 5, pp. 334–343, 2008.

[31] A. F. Bingöl and R. Gül, "Residual bond strength between steel bars and concrete after elevated temperatures," *Fire Saf. J.*, vol. 44, no. 6, pp. 854–859, 2009.

[32] H. Ş. Arel and Ş. Yazıcı, “Effect of different parameters on concrete-bar bond under high temperature,” *ACI Mater. J.*, vol. 111, no. 6, pp. 633–639, Dec. 2014.

[33] A. Ergün, G. Kürklü, and M. S. Başpınar, “The effects of material properties on bond strength between reinforcing bar and concrete exposed to high temperature,” *Constr. Build. Mater.*, vol. 112, pp. 691–698, Jun. 2016.

[34] E. Lublóy and V. Hlavička, “Bond after fire,” *Constr. Build. Mater.*, vol. 132, pp. 210–218, Feb. 2017.

[35] F. B. Varona, F. J. Baeza, D. Bru, and S. Ivorra, “Evolution of the bond strength between reinforcing steel and fibre reinforced concrete after high temperature exposure,” *Constr. Build. Mater.*, vol. 176, pp. 359–370, Jul. 2018.

[36] J. Lee, E. Sheesley, Y. Jing, Y. Xi, and K. Willam, “The effect of heating and cooling on the bond strength between concrete and steel reinforcement bars with and without epoxy coating,” *Constr. Build. Mater.*, vol. 177, pp. 230–236, Jul. 2018.

[37] O. Yang, B. Zhang, G. Yan, and J. Chen, “Bond performance between slightly corroded steel bar and concrete after exposure to high temperature,” *J. Struct. Eng.*, vol. 144, no. 11, pp. 04018209-1–10, Nov. 2018.

[38] A. Windisch, “A modified pull-out test and new evaluation methods for a more real local bond-slip relationship,” *Mater. Struct.*, vol. 18, no. 105, pp. 181–184, 1985.

[39] F. Aslani and B. Samali, “Predicting the bond between concrete and reinforcing steel at elevated temperatures,” *Struct. Eng. Mech.*, vol. 48, no. 5, pp. 643–660, 2013.

[40] European Committee for Standarisation, *UNE-EN 12390-3:2009 Testing hardened concrete - Part 3: Compressive strength of test specimens*. Madrid, 2009.